Supplementary Material

Band excitation piezoresponse force microscopy adapted for weak ferroelectrics: On-the-fly tuning of the central band frequency

Maxim Spiridonov, Anastasia Chouprik, Vitalii Mikheev, |*

Andrey M. Markeev, and Dmitrii Negrov

Moscow Institute of Physics and Technology,

9 Institutskiy lane, Dolgoprudny, Moscow Region, 141700, Russia

* chouprik.aa@mipt.ru

Section S1. Postprocessing of spectra with low SNR by signal filtering or principal component analysis (PCA)

The data postprocessing also allows to decrease the measurement rate. The choice of optimal postprocessing approach depends on the stability of the employed algorithm of response fitting. For a stable algorithms (for example, the vector fitting technique, Gustavsen & Semlyen, 1999) the applying of routine low-pass filter (for example, Butterworth filter) is sufficient. Indeed, whereas for the raw response with low SNR (green line in Figure S1) algorithm get into local minimum during initial evaluation and fit a some spike by Lorentz curve with non-physically high quality factor Q = 69 000 (orange line), the filtering (black line) allow to fit a spectra using the same algorithm by the curve with Q = 84 (cherry line).

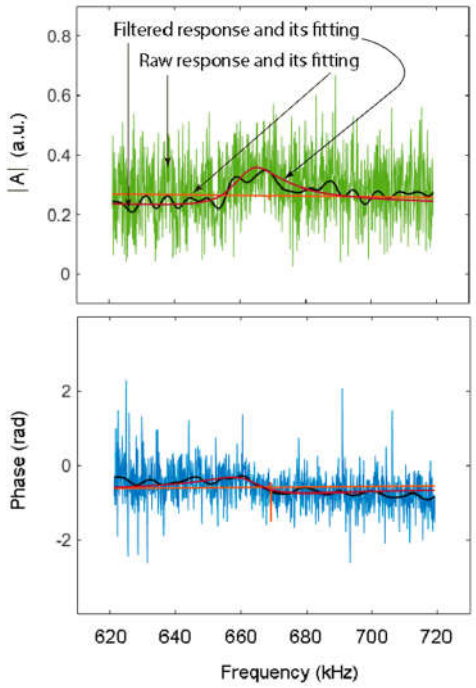

Figure S1. Results of low-pass filtering applied to raw spectra.

For not very stable fitting algorithms, multivariate statistical analysis methods such as the principal component analysis (PCA) (Bonnet, 1998) are preferable. PCA separates data into orthonormal components (eigenvectors) arranged in ascending order of eigenvalue. Usually, the statistically relevant information about the spectral response is in a few eigenvectors, whereas the rest ones correspond to noise. Spectrum of four informative components (marked in Figure S2) determined over 9200 spectrum could be fitted by any algorithm. The spectrum of seven components is very similar to the one of four component thus indicating the sufficiency of only

four components. The disadvantage of PCA processing is non-possibility of on-the-fly PFM imaging, because a large dataset is required.

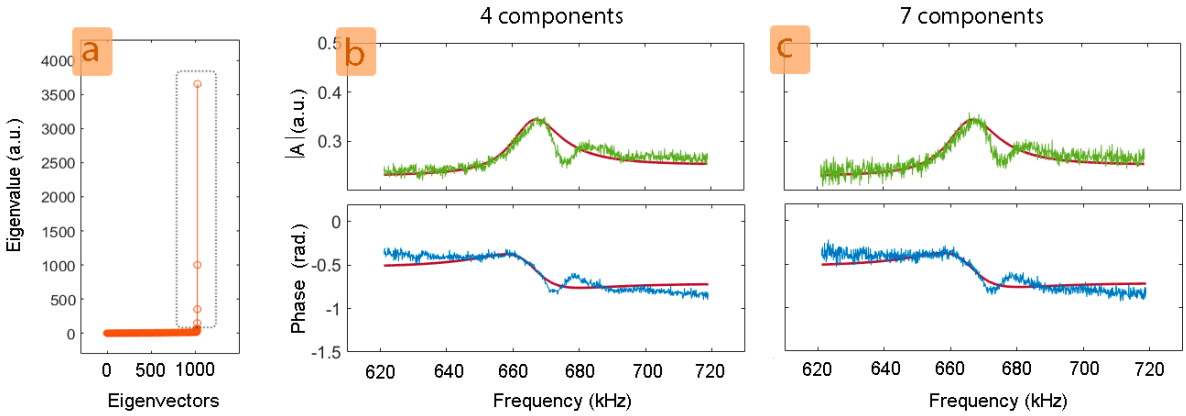

Figure S2. Results of principal component analysis (PCA) applied to raw spectra in Figure S1: (a) PCA Scree plot; the informative components are marked; the spectra of four (b) and seven (c) informative components.

Section S2. Background of AFM Ntegra

In measurements of the piezoresponse with low signal-to-noise ratio, the background of AFM setup can significantly contribute to the result of measurement, changing the magnitude of piezoresponse and rotating the phase. Every AFM setup has its own peculiar background. In this work, AFM Ntegra (NT-MDT) of early (2008) edition with a universal measuring head was used. The background was acquired by the averaging of the absolute amplitude spectra in the range 0-

1.6 MHz (Figure S3). At the averaging of 1000-2000 spectra the contact thermal peak is also observed.

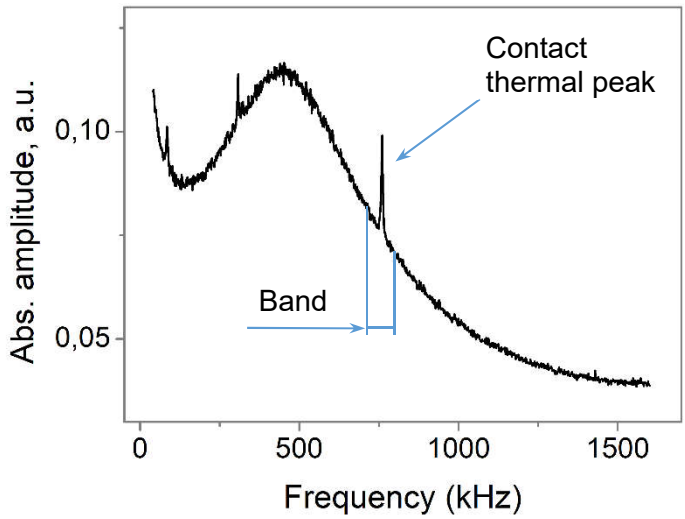

Figure S3. Wide-band spectrum of the background of AFM Ntegra.

Note that in the range of band 100 kHz the background can be approximated by the linear dependence on frequency for any contact resonance frequency.

Section S3. Qualitative comparison of PFM techniques

As it is shown in the paper, standard deviation of PFM phase $\sigma_\varphi = \sqrt{\mathrm{var}(\varphi)}$ over monodomain ferroelectric characterizes the width of the phase distribution, and it can serve as a quantitative criteria of both the precision of PFM techniques and the quality of the PFM image under the same experimental conditions (experimental setup and peak-to-peak value of excitation voltage).

In Figure S4 the phase distribution and the standard deviations of phase over monodomain capacitor W/$Hf_{0.5}Zr_{0.5}O_2$/TiN studied by classical BE, narrow-band BE with the tuning of the central band frequency and off-resonance single frequency PFM are shown (Figure S4a). Due to polycrystallinity and polymorphism of $Hf_{0.5}Zr_{0.5}O_2$ films, some deviation of PFM amplitude exists in maps (Fig. S4b-S4f). Dark amplitude regions are associated with the grains of non-ferroelectric phase, misaligned ferroelectric phase and the seeds of the domains with opposite polarization (simulation of the resolution of PFM studies in capacitor geometry was performed earlier in Chouprik et al., 2019). To eliminate the contribution of the phase deviations due to such regions,

the calculation of phase standard deviation were performed only over the map points corresponded to the amplitude that was larger some threshold amplitude.

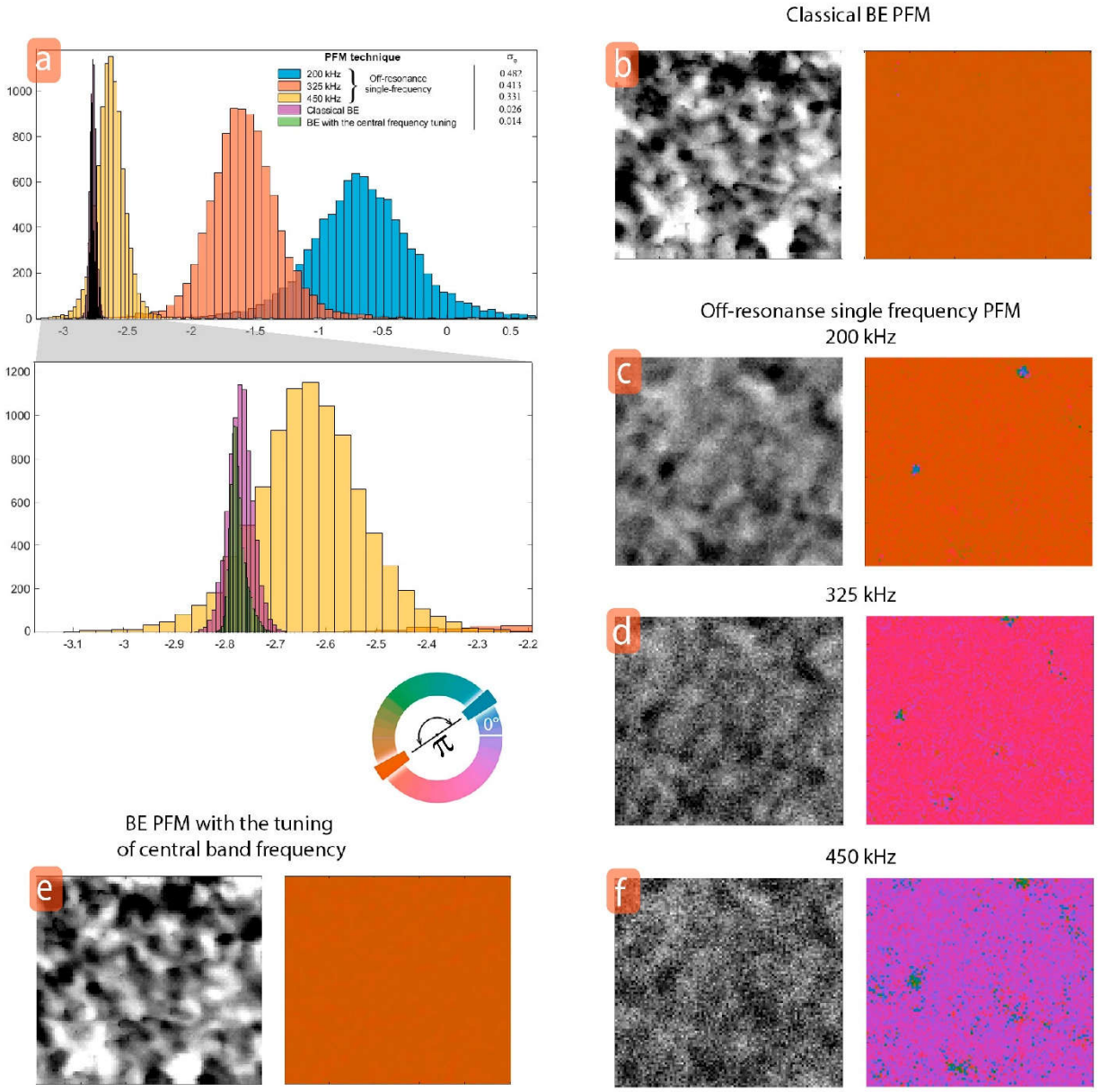

Figure S4. Histograms of PFM phase over monodomain capacitor W/$Hf_{0.5}Zr_{0.5}O_2$/TiN for three techniques (a) and an appropriate PFM amplitude and phase maps (b)-(f) acquired during the same time.

It is obvious that σ_φ for the off-resonance single frequency maps is significantly larger than σ_φ for both BE techniques. The mean average value for 200, 325, 450 kHz corresponds to an appropriate phase value on $\varphi(f)$ curve of cantilever oscillation system.

References

Bonnet, N. (1998) Multivariate statistical methods for the analysis of microscope image series: applications in materials science, *J Microsc-Oxford* **190**, 2-18.

Chouprik, A., Spiridonov, M., Zarubin, S., Kirtaev, R., Mikheev, V., Lebedinskii, Yu., Zakharchenko, S., Negrov, D. (2019) Wake-up in a $Hf_{0.5}Zr_{0.5}O_2$ film: a cycle-by-cycle emergence of the remnant polarization via the domain depinning and the vanishing of the anomalous polarization switching, *ACS Appl. Electron. Mater.* **1** (3) (2019) 275.

Gustavsen, B. & Semlyen A. (1999) Rational approximation of frequency domain responses by vector fitting, in *IEEE Transactions on Power Delivery*. **14** 3.